



Fermi National Accelerator Laboratory

FERMILAB-Conf-96/198-E

CDF

**Measurement of the B Meson Differential Cross-Section in $p\bar{p}$
Collisions at $\sqrt{s} = 1.8$ TeV**

A. Laasanen et al.

For the CDF Collaboration

*Fermi National Accelerator Laboratory
P.O. Box 500, Batavia, Illinois 60510*

July 1996

Contributed Paper at the *28th International Conference on High Energy Physics (ICHEP96)*,
Warsaw, Poland, July 25-31, 1996

Disclaimer

This report was prepared as an account of work sponsored by an agency of the United States Government. Neither the United States Government nor any agency thereof, nor any of their employees, makes any warranty, expressed or implied, or assumes any legal liability or responsibility for the accuracy, completeness, or usefulness of any information, apparatus, product, or process disclosed, or represents that its use would not infringe privately owned rights. Reference herein to any specific commercial product, process, or service by trade name, trademark, manufacturer, or otherwise, does not necessarily constitute or imply its endorsement, recommendation, or favoring by the United States Government or any agency thereof. The views and opinions of authors expressed herein do not necessarily state or reflect those of the United States Government or any agency thereof.

**Measurement of the B Meson Differential Cross-Section
in $p\bar{p}$ Collisions at $\sqrt{s} = 1.8$ TeV**

The CDF Collaboration

This paper presents a direct measurement of the differential B^+ and B^0 cross-sections, $d\sigma/dp_T$, in $p\bar{p}$ collisions at $\sqrt{s} = 1.8$ TeV using a sample of $74 pb^{-1}$ accumulated by the Collider Detector at Fermilab(CDF). The cross-sections are measured in the central pseudorapidity region $|\eta| < 1$ for $p_T(B) > 6.0$ GeV/c by fully reconstructing the B meson decays $B^+ \rightarrow J/\psi K^+$ and $B^0 \rightarrow J/\psi K^{*0}(892)$, where $J/\psi \rightarrow \mu^+ \mu^-$ and $K^{*0} \rightarrow K^+ \pi^-$. The prediction of next-to-leading order QCD is consistent with the shape of the differential cross-section but is low by a factor of $2.1 \pm 0.2 \pm 0.3$. The integrated B meson cross-section for $p_T(B) > 6.0$ GeV/c is determined to be $\sigma(B^-) = 2.54 \pm 0.22 \pm 0.53 \mu b$.

The prediction of QCD theory was in agreement with the first b quark cross-section measurements in $p\bar{p}$ collisions which were made by UA1 at $\sqrt{s} = 630$ GeV [1]. Initial measurements made at $\sqrt{s} = 1.8$ TeV at the Collider Detector at Fermilab (CDF) [2,4] cast doubt on whether QCD correctly predicts either the absolute rate or shape of the transverse momentum (p_T) distribution, whereas a measurement made more recently at the D0 detector [14] at the same center-of-mass energy is in agreement with the QCD prediction. We previously presented [13] the first direct measurement of the B meson differential cross-section $d\sigma/dp_T$ in hadronic collisions by measuring the mass and momentum of the B mesons decaying into exclusive final states. The differential cross-section so obtained provides a test of the QCD prediction that is complementary to measurements which infer the b quark content and momentum distribution from an inclusive lepton spectrum after unfolding contributions

from both b and c quarks. The data sample used represented $19.3 \pm 0.8 \text{ pb}^{-1}$ collected by CDF during the 1992-93 run. B mesons were reconstructed via the decays $B^+ \rightarrow J/\psi K^+$ and $B^0 \rightarrow J/\psi K^{*0}(892)$, with $J/\psi \rightarrow \mu^+ \mu^-$ and $K^{*0} \rightarrow K^+ \pi^-$, and their charge conjugates. This analysis found the shape of the B meson differential cross-section was adequately described by next-to-leading order QCD but the absolute rate was at the limits of that predicted by typical variations in the theoretical parameters. Here we extend that analysis by incorporating an additional $54.4 \pm 5.4 \text{ pb}^{-1}$ of data taken in the $B^+ \rightarrow J/\psi K^+$ channel during the 1994-95 running period. The $B^0 \rightarrow J/\psi K^{*0}$ channel has not yet been analyzed for the 1994-95 data. Detailed descriptions of the CDF detector have been provided elsewhere [5]. The components relevant to this analysis are briefly described here. The z -axis of the detector coordinate system is along the beam direction. The Central Tracking Chamber (CTC) is a drift chamber in a 1.4T axial magnetic field, consisting of nine superlayers, four of which give stereo information. A particle must have pseudorapidity $|\eta| < 1$ to pass through all nine superlayers, which defines the rapidity range used for the cross-section measurement.

A Silicon Vertex Detector (SVX) provides high-resolution $r - \phi$ tracking information near the interaction region [6]. The SVX detector is 51 cm long and consists of four layers of silicon microstrip detectors with an innermost radius of 3.0 cm. Pattern recognition is done by extrapolating tracks from the CTC. Surrounding the CTC are electromagnetic and hadronic calorimeters, outside of which are the central muon chambers, segmented into 72 modules which provide about 85% coverage in azimuth in the pseudorapidity range $|\eta| < 0.6$. For the 1994-95 run the muon detection was improved by adding additional absorber and detectors outside the central muon chambers and extending the η coverage to $|\eta| < 1.0$. The analysis of the 1994-95 data described below is very similar to the published 1992-93 analysis. The selection of B candidates begins by identifying J/ψ candidates which decay to two muons. There are three levels of trigger requirements that must be satisfied for a muon pair to be included in the J/ψ data sample. At the first trigger level, the muons must have been detected in the muon chambers and pass a minimal transverse requirement of $\sim 1.4 \text{ GeV}/c$. Prompt muons with lower momenta range out in the calorimeters. At the second

trigger level, either one or both of the muon chamber tracks depending upon the particular trigger type must match a track found in the CTC by a hardware track processor. Several different dimuon triggers were used and the events were required to pass at least one of them. These triggers differed in the p_T threshold, in the number of matching muon tracks required and the specific muon detector in which they were found. Some of the triggers were prescaled. At the third (software) trigger level, detailed CTC pattern recognition and tracking are done.

To improve the purity of the J/ψ sample, the CTC track is required to match its associated muon chamber track to within 3σ in $r - \phi$ and 3.5σ in z . To match the trigger thresholds, each muon is either required to have $p_T \geq 1.8$ GeV/c, and at least one muon is required to have $p_T \geq 2.8$ GeV/c or else both muons are required to have $p_T \geq 2.0$. The former cuts were used in the 1992-93 run and the latter for most triggers during the 1994-95 run. The invariant mass and uncertainty σ_m are calculated for each muon pair. The signal region is defined to be those dimuon candidates with invariant masses within $4\sigma_m$ of the known J/ψ mass [15]. The K^+ candidates are required to have $p_T > 1.25$ GeV/c.

We find the B -candidate mass and momentum subject to the constraint that the decay tracks come from a common vertex and the invariant mass of the dimuon tracks is equal to the J/ψ mass. We require the confidence level of the fit to be greater than 0.5%. The transverse momentum for each B candidate is required to be greater than 6.0 GeV/c, the minimum p_T required to produce decay products satisfying the trigger and selection requirements. The proper decay length $c\tau \equiv L_{xy}m_B/p_T$ is calculated, where L_{xy} is the projection of the B vertex displacement onto the B transverse momentum. About 75% of the background that occurs when a prompt J/ψ is combined with other tracks from the primary vertex is removed by requiring $c\tau$ to be greater than $100 \mu m$.

The B candidates are divided into subsamples in p_T ranges 6-9, 9-12, 12-15, and 15-20 GeV/c. For each p_T range, the invariant mass distributions are fit to a Gaussian plus linear background using an unbinned likelihood method. The mass range below $5.2 \text{ GeV}/c^2$ is excluded from the fits since it can include contributions from higher multiplicity B decay

modes. The B^+ invariant mass distributions from the new 1994-95 data for each momentum range are shown in figures 1 through 4, and the fitted numbers of events are given in table I.

The B -meson differential cross-section is calculated from

$$\frac{d\sigma(B)}{dp_T} = \frac{N}{2 \cdot \mathcal{L} \cdot A \cdot e \cdot F \cdot \Delta p_T} \quad (1)$$

where N is the number of events observed, \mathcal{L} is the integrated luminosity, A is the detector acceptance (including the efficiency of the kinematic cuts), e is the combined tracking and track-matching efficiency, F is the branching fraction, and Δp_T is the width of the p_T bin. The factor of 1/2 is included because decays involving both B and \bar{B} mesons have been reconstructed, but the quoted cross-sections are for B mesons only.

A Monte Carlo simulation employing the next-to-leading order QCD calculation [7] with renormalization scale $\mu = \sqrt{m_b^2 + p_T^2}$, the MRSD₀ proton structure functions [8], the Peterson parameterization [9] for fragmentation, using a value of the fragmentation parameter of 0.006, and a detector and J/ψ trigger simulation was used to determine the acceptance, shown in table I.

Product branching fractions of $(6.55 \pm 1.01) \times 10^{-5}$ and $(6.67 \pm 1.21) \times 10^{-5}$ [10] were used for the $B^+ \rightarrow J/\psi K^+$ and $B^0 \rightarrow J/\psi K^{*0}$ decays, which include the J/ψ and the K^{*0} branching ratios.

Varying the b quark mass and the QCD renormalization scale used in the Monte Carlo simulation within their uncertainties changes the calculated acceptance by $\pm 2\%$ [11]. The systematic uncertainty in the J/ψ efficiency due to the trigger parameterization was determined to be $\pm 4\%$. Additionally, a systematic uncertainty of $\pm 4\%$ is associated with the reconstruction of kaons which decay inside the CTC volume. The efficiency of the $100\mu m$ cut on $c\tau$ has an uncertainty of $\pm 4\%$, due to its dependence on the lifetime of the meson and the $c\tau$ resolution, which varies from 25 to 500 μm , depending on whether or not SVX information was available for the vertex fit. The χ^2 requirement on the common-vertex constraint has an additional 1% uncertainty, which was determined from the fraction of J/ψ

which fail such a requirement. The total reconstruction efficiency is $(74.6 \pm 3.8)\%$ for the B^+ decay.

The 1994-95 differential cross-sections are in good agreement with the previous results from the 1992-93 run. The combined 1992-93 B^+ and B^0 and the 1994-95 B^+ meson cross-sections, $\frac{d\sigma(B)}{dp_T}$, are listed in table I and plotted in figure 5, where the common branching ratio uncertainty (included in table I) is shown separately. The $p_T = 17.2$ GeV/c point comes from the 1994-95 data while the $p_T = 20.0$ GeV/c point comes solely from the 1992-93 data. The solid curve in figure 5 shows the B meson differential cross-section predicted by the QCD-based Monte Carlo simulation as described above, while the dashed curves indicate the variation associated with uncertainty in the b quark mass, the fragmentation parameter and the renormalization scale [16]. The curves include the generally used assumption that 75% of \bar{b} quarks fragment in equal amounts to B^+ and B^0 mesons [3,12]. The visual comparison between data and theory is aided by plotting (data/QCD) on a linear scale as shown in figure 6. To determine the level of agreement between the data and the theoretical prediction, the ratio (data/QCD) is fit to a horizontal line. The fit yields an overall scale factor of $2.1 \pm 0.2 \pm 0.3$ with a confidence level of 21%. The integrated B meson cross-section above 6 GeV/c is determined to be $2.54 \pm 0.22 \pm 0.53$.

In conclusion, we find that the shape of the B meson differential cross-section presented here is consistent with next-to-leading order QCD but the absolute rate predicted by theory is low by a factor of $2.1 \pm 0.2 \pm 0.3$.

We thank the Fermilab staff and the technical staffs of the participating institutions for their vital contributions. This work was supported by the U.S. Department of Energy and National Science Foundation; the Italian Istituto Nazionale di Fisica Nucleare; the Ministry of Education, Science and Culture of Japan; the Natural Sciences and Engineering Research Council of Canada; the National Science Council of the Republic of China; and the A. P. Sloan Foundation.

1. C. Albajar *et al.*, UA1 Collab., Phys. Lett. B **186**, 237 (1987); **213**, 405 (1988); **256**,

- 121 (1991).
2. F. Abe *et al.*, CDF Collab., Phys. Rev. Lett. **71**, 500 (1993); **71**, 2396 (1993); **68**, 3403 (1992); Phys. Rev. D **50**, 4252 (1994).
 3. F. Abe *et al.*, CDF Collab., Phys. Rev. Lett. **68**, 3403 (1992); Phys. Rev. D **50**, 4252 (1994).
 4. F. Abe *et al.*, CDF Collab., Phys. Rev. Lett. **69**, 3704 (1992); **71**, 2537 (1993). These papers underestimated direct J/ψ and $\psi(2S)$ production.
 5. F. Abe *et al.*, CDF Collab., Nucl. Instrum. Methods Phys. Res., Sect. A **271**, 387 (1988).
 6. D. Amidei *et al.*, Nucl. Instrum. Methods Phys. Res., Sect. A **350**, 73 (1994).
 7. P. Dawson *et al.*, Nucl. Phys. **B327** (1988) 49; M. Mangano *et al.*, Nucl. Phys. **B373** (1992) 295.
 8. A. Martin, R. Roberts and J. Stirling, RAL-92-021, DTP/92/16 (1992).
 9. C. Peterson *et al.*, Phys. Rev. D **27**, 105 (1983); J. Chrin, Z. Phys. C **36**, 163 (1987).
 10. M.S. Alam *et al.*, CLEO Collab., Phys. Rev. D **50** (1994) p. 43.
 11. M. W. Bailey, Ph.D. thesis, Purdue University, 1994.
 12. B. Adeva *et al.*, L3 Collab., Phys. Lett. B **252** (1990), 703; D. Decamp *et al.*, ALEPH Collab., Phys. Lett. B **258** (1990), 236; H. C. Albajar *et al.*, UA1 Collab., Phys. Lett. B **262** (1991), 171; F. Abe *et al.*, CDF Collab., Phys. Rev. Lett. **67**, 3351 (1991).
 13. F. Abe *et al.*, CDF Collab., Phys. Rev. Lett. **75**, 1451 (1995).
 14. S. Abachi *et al.*, D0 Collab., Phys. Rev. Lett. **74**, 3548 (1995).
 15. M. Aguilar-Benitez *et al.*, Phys. Rev. D **50**, 1173 (1994).
 16. The b quark mass is varied between 4.5 and 5.0 GeV/c², the renormalization scale is varied between $\mu_0/2$ and $2\mu_0$, and the fragmentation parameter is varied between 0.004 and 0.008.

TABLE I. Differential B meson cross-section, $d\sigma(|y| < 1.0)/dp_T$ (nb/GeV/c). The 1994-95 cross-sections include only charged B mesons while the combined 1992-93 and 1994-95 cross-sections include in addition B^0 's from 1992-93. The uncertainties shown for the number of events are statistical; the systematic uncertainty has been included in the cross-section uncertainty.

$\langle p_T \rangle$ (GeV/c)	Events	Acceptance (%)	$d\sigma(y < 1.0)/dp_T$ (1994-95) (nb/GeV/c)	$d\sigma(y < 1.0)/dp_T$ (combined) (nb/GeV/c)
7.4	140 ± 22	1.44 ± 0.02	$610 \pm 96 \pm 128$	$603 \pm 70 \pm 127$
10.4	105 ± 14	3.91 ± 0.06	$168 \pm 22 \pm 35$	$144 \pm 16 \pm 30$
13.4	69 ± 10	6.69 ± 0.12	$65 \pm 9 \pm 14$	$60 \pm 7 \pm 13$
17.2	52 ± 7	9.18 ± 0.19	$21 \pm 3 \pm 4$	$21 \pm 3 \pm 4$
20.0				$7.2 \pm 1.4 \pm 1.8$

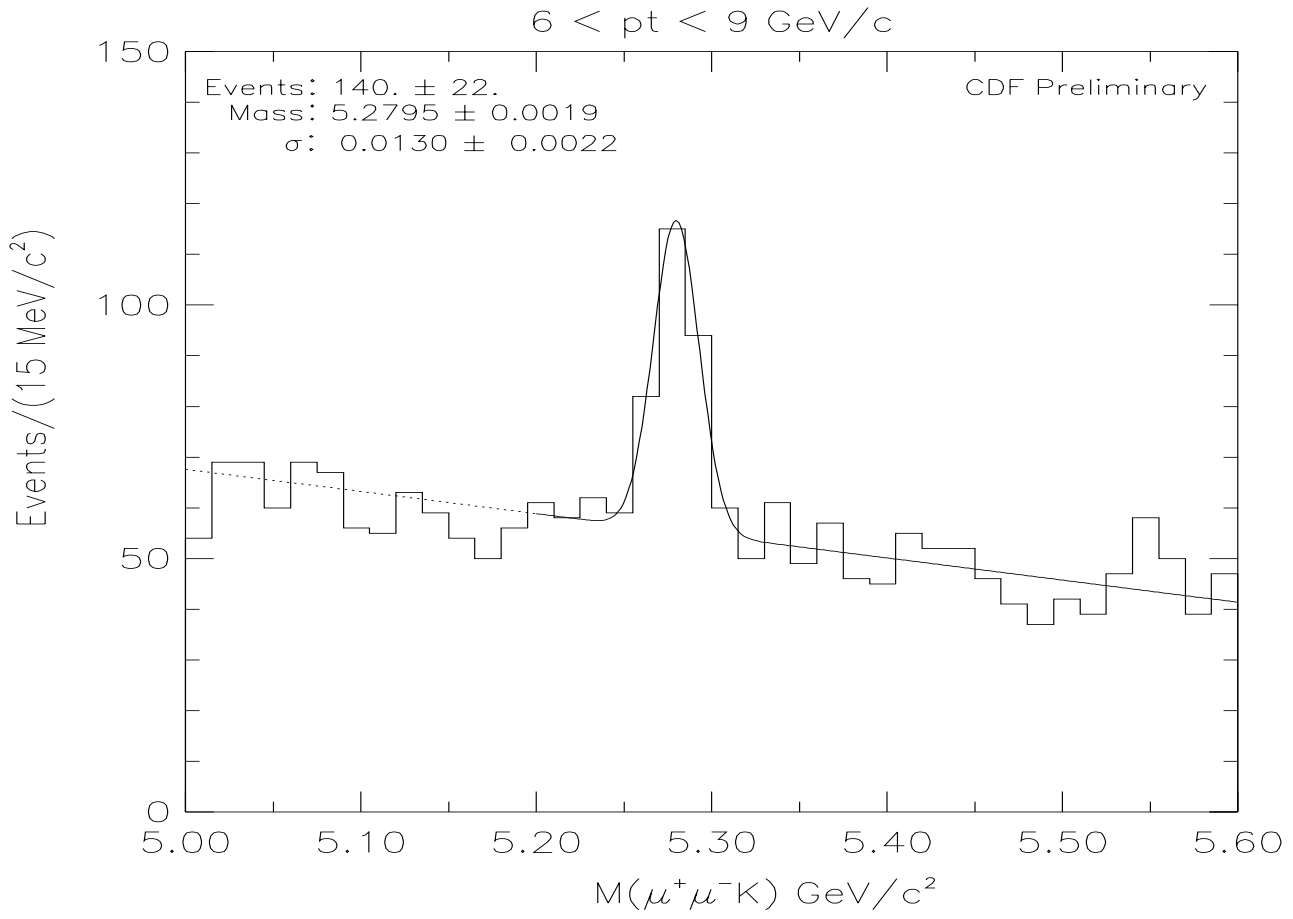


FIG. 1. B^\pm meson invariant mass distributions for the momentum range 6-9 GeV/c.

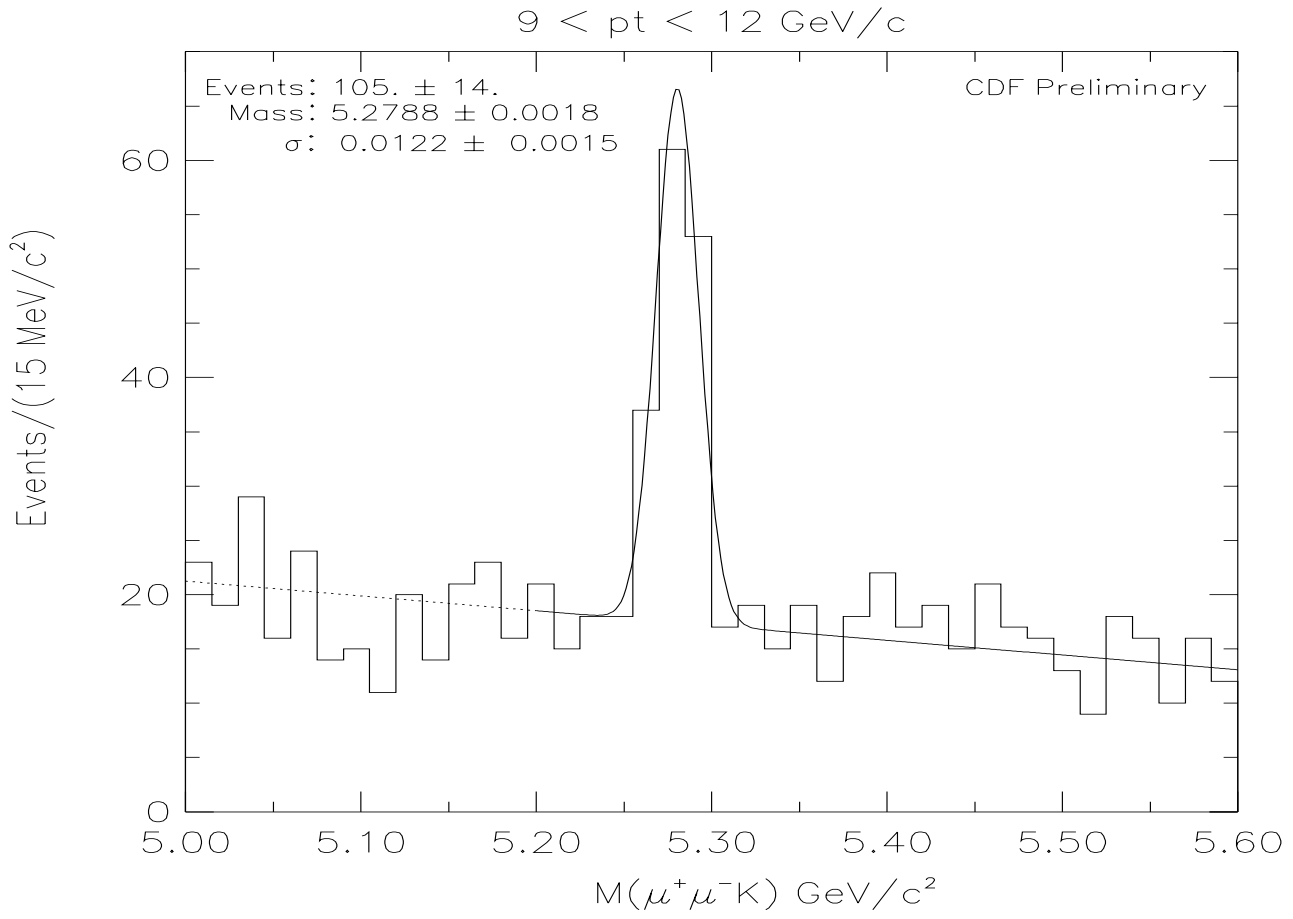


FIG. 2. B^\pm meson invariant mass distributions for the momentum range 9-12 GeV/c.

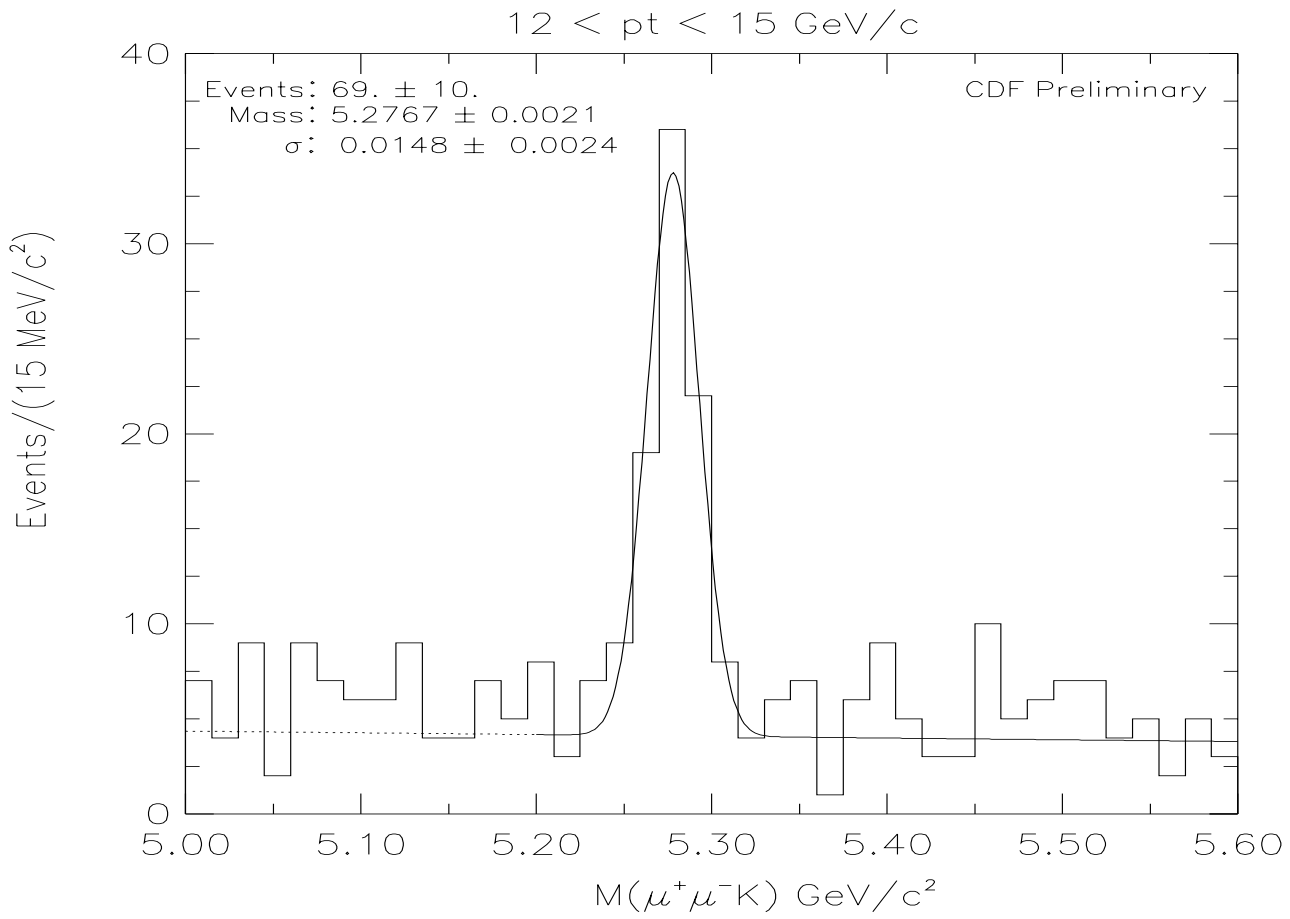


FIG. 3. B^\pm meson invariant mass distributions for the momentum range 12-15 GeV/c.

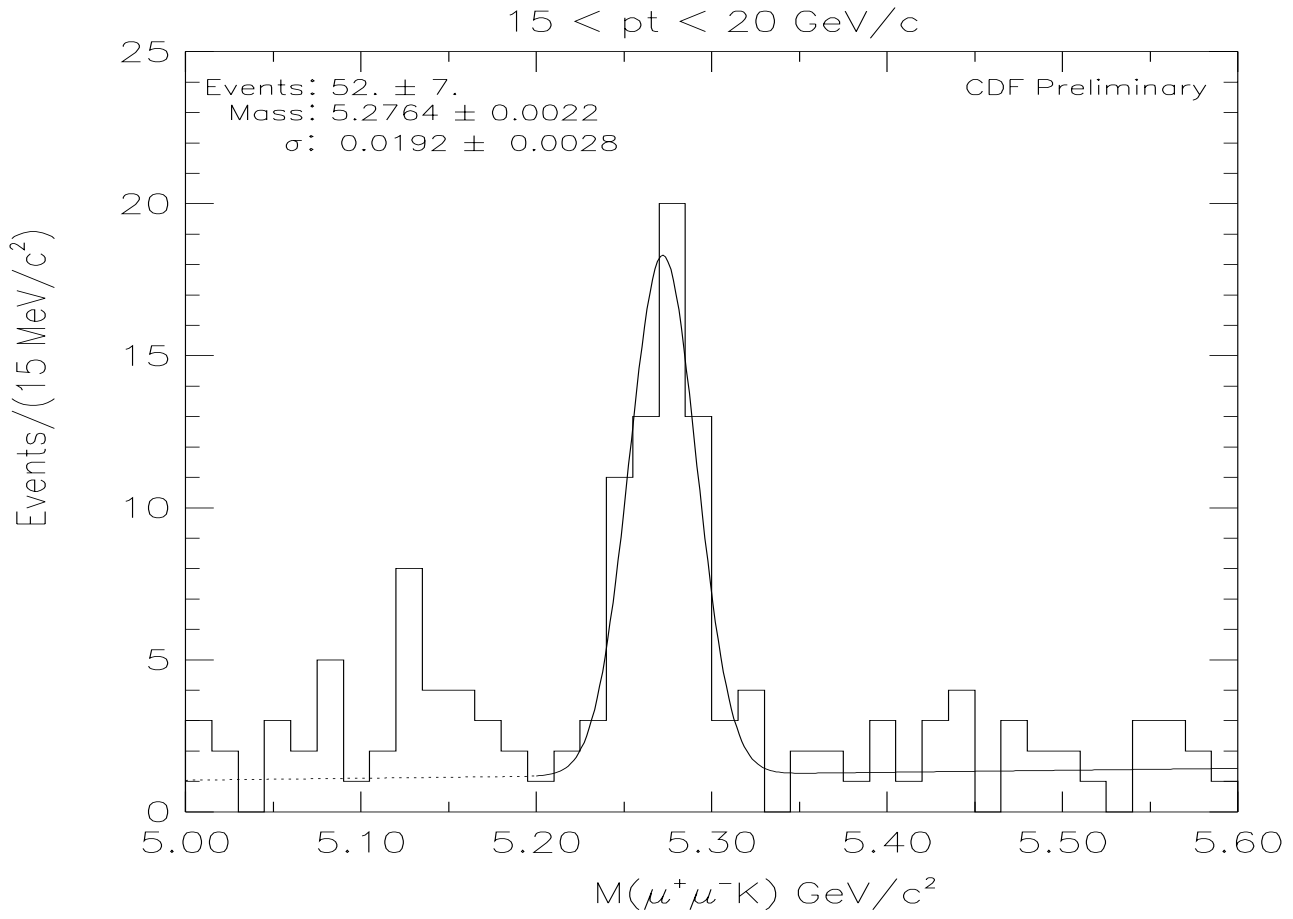


FIG. 4. B^\pm meson invariant mass distributions for the momentum range 15-20 GeV/c.

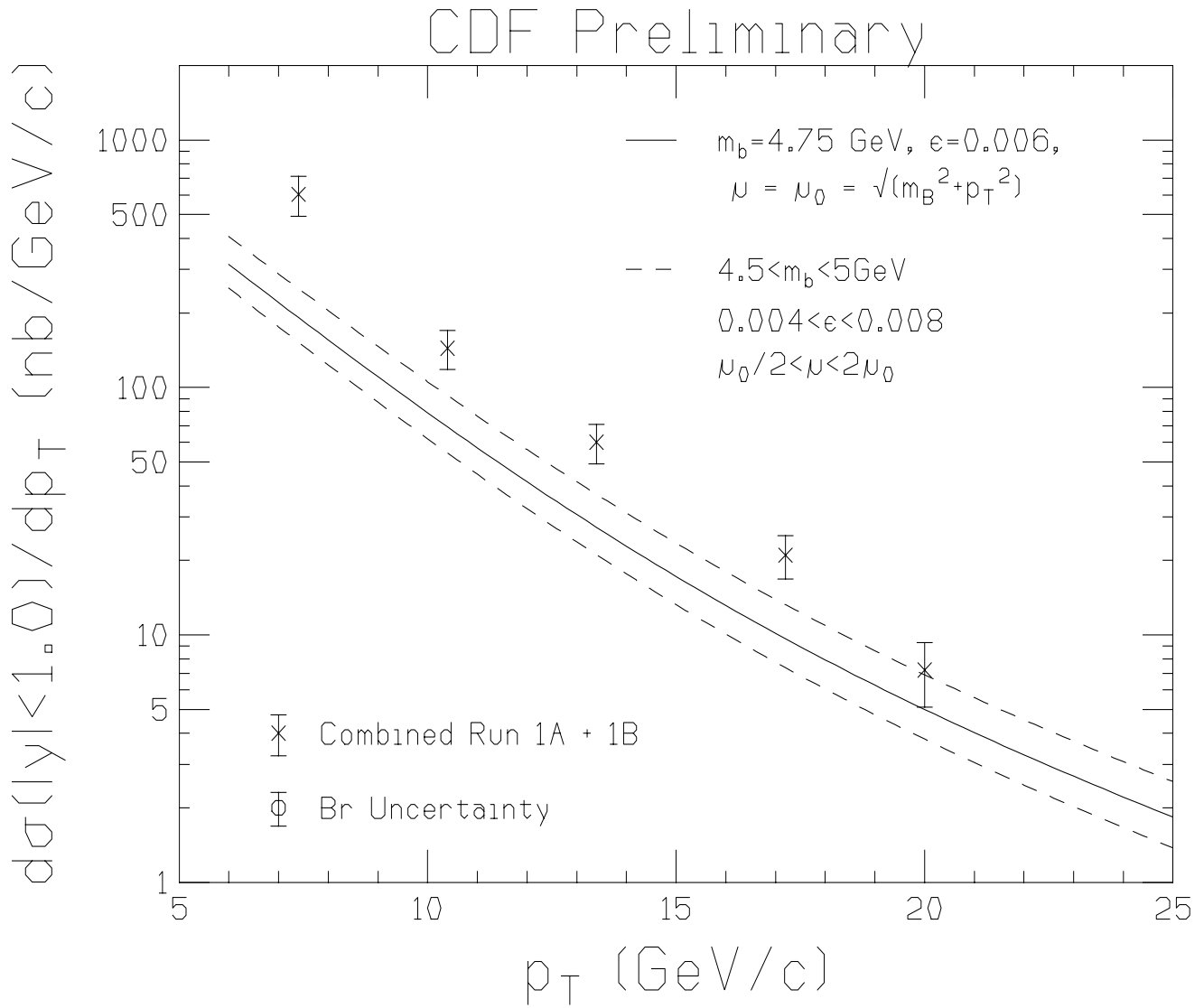


FIG. 5. B meson differential cross-sections compared to the QCD prediction. The branching ratio uncertainty is shown separately.

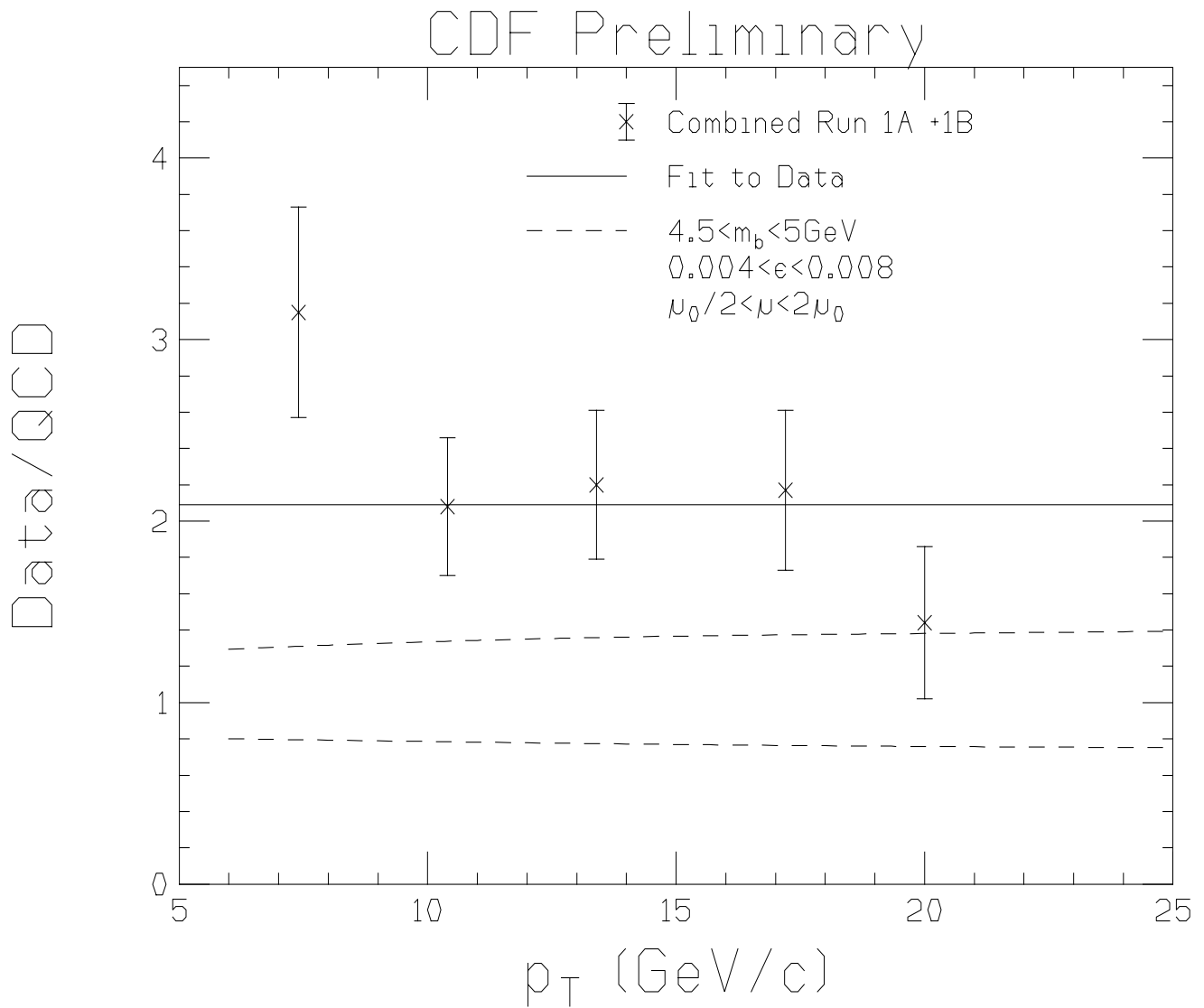


FIG. 6. The ratio data/QCD. The branching ratio uncertainty is not included in the errors.